19th International Conference on
Adaptive Structures and Technologies
October 6-9, 2008
Ascona, Switzerland

A second-order controller for resonance damping and tracking control of nanopositioning systems

Sumeet S. Aphale[1], Andrew J. Fleming[2] and S. O. R. Moheimani[3]*
[1] Centre for Applied Dynamics Research (CADR), School of Engineering, Kings College, University of Aberdeen, UK.
[2] ARC Center of Excellence for Complex Dynamic Systems and Control, University of Newcastle, Callaghan, Australia
[3]* School of Electrical Engineering and Computer Science, The University of Newcastle, Callaghan, NSW, Australia
(Corresponding Author: reza.moheimani@newcastle.edu.au)

ABSTRACT

This paper presents a simple second-order controller that damps the resonance typical of piezoelectric nanopositioners and delivers good tracking performance. This method employs the Integral Resonant Control scheme (IRC) for damping the dominant resonant mode of the piezoelectric nanopositioner and uses an integral controller to achieve tracking performance. As disturbance rejection is a main concern in nanopositioning applications, the control scheme is tested for its disturbance rejection performance. It is seen that the control scheme has good disturbance rejection characteristics deeming it suitable for nanopositioning applications. To test the tracking performance, the system is made to track a 20 Hz triangular input at various integral gains. It is shown that improved tracking performance can be achieved at high gains with only a slight degradation in disturbance rejection performance at high frequencies.

Keywords: Nanopositioning, vibration control, tracking

1. INTRODUCTION

Nanopositioning devices and strategies have generated a significant amount of interest in the recent years, mainly due to their impact on areas such as MEMS, scanning probe microscopy and nanolithography [1, 2, 3, 4]. Piezoelectric stack-actuated nanopositioners are well-suited for this particular application due to their simple construction, ease of control, large motion ranges and low cross-coupling. This has generated a lot of interest in the design and control of various nanopositioners [5, 6, 7]. Various designs of piezoelectric stack actuated nanopositioning platforms are commercially available today [8, 9]. The main concern in using these nanopositioners is their dominant resonant mode which exists at relatively low frequencies [10]. This resonant mode reduces the positioning bandwidth of the nanopositioner greatly.

Strategies that effectively damp the resonance of such systems have been documented in the past. Passive damping techniques such as shunts have been reported but they need constant tuning and show a drastic performance degradation if the resonance changes, thus, adaptive shunts that handle system uncertainties have been researched [11, 12]. Earlier researchers have documented various feedback controllers that impart substantial damping to the resonant system [13, 14, 5, 15]. Resonant control [16] and Positive Position Feedback control (PPF) [17] have been investigated for their substantial damping performance. The polynomial-based controller is another simple damping controller design that has been tested on various systems [18, 19, 20]. Need of an accurate system model, lack of robustness under changes in resonance frequencies and higher order control designs are some of the drawbacks that the aforementioned techniques may suffer from. Integral resonant

control (IRC) has shown the capability of damping multiple modes of a collocated system without any instability issues due to unmodeled dynamics [21]. The ease of design, controller simplicity and its low order (usually first order) are some of the favorable characteristics of the IRC technique.

Open- and closed-loop tracking algorithms for nanopositioning applications have also been proposed in the past. Inversion-based feedforward techniques for continuously tracking a desired periodic trajectory have been under investigation [22, 23]. Inversion-based feedforward technique has also been applied to nanopositioning systems [24]. This approach has also been applied to compensate for nonlinear effects such as creep and hysteresis [25, 26]. The main drawback of the feedforward control strategy is its high sensitivity to modeling errors and plant parameter uncertainties. Feedback has been shown to improve the bandwidth of feedforward strategies by reducing the effects of uncertainties [27]. Robust tracking was reported in [28]. Force-feedback for nanomanipulation was reported in [29]. H_∞ control algorithms for nano-scale tracking have also been investigated [30]. A detailed review of various control strategies for nanopositioning applications can be found in [31].

Feedback approach combining a damping controller that renders the system insensitive to variations in resonance frequency with a Proportional Integral controller (PI) has been reported earlier [10]. The high gain needed by the integrator to track a given trajectory limits the achievable scan speeds. Similarly, feedback/feedforward technique to achieve damping and tracking has also been reported [32]. Both these methods require a plant model for their control design. Also, the overall controller order is three in case of the feedback algorithm while in case of the feedback/feedforward strategy, there is added computational cost and complexity due to the identification, modeling and inversion of the closed-loop system. In this work, we present a way to integrate the IRC scheme with a PI controller to achieve both damping and tracking performance. It will also be shown that this implementation will improve the disturbance rejection pro file of the nanopositioner, a highly desirable outcome for nanopositioning-type applications.

1.1 Outline

The experimental setup is described Section II. Section III will describe the proposed control strategy. The damping control and the tracking control design are described in its subsections. Details of the implemented IRC scheme for damping and the PI controller for tracking are given in Section IV. Experimental results for tracking a 20 Hz triangle wave validate the proposed control scheme an are also presented in Section IV. Section V concludes the article.

1.2. Objectives

The main objective of this work is to damp the low frequency resonant mode of a commercially available piezoelectric nanopositioner and achieve tracking performance. The transfer function from the driving voltage input to the displacement output of the platform is collocated due to the fashion in which the capacitive sensors are placed. This makes the IRC scheme a perfect choice as a damping control technique. It will be shown that by implementing the IRC and the integral tracking controller in a specific fashion, both tracking and disturbance rejection can be achieved. A PI-734 nanopositioning platform (by Physik Instrumente) is a popular commercially available nanopositioning platform that exhibits a sharp resonant peak at relatively low frequencies ($\approx$ 400 Hz). It is susceptible to high amplitude vibrations when disturbed and will be used to experimentally validate the theories presented in this work. Experimental results will show that good damping and tracking performance can be obtained by this scheme whilst maintaining a desirable disturbance rejection profile.

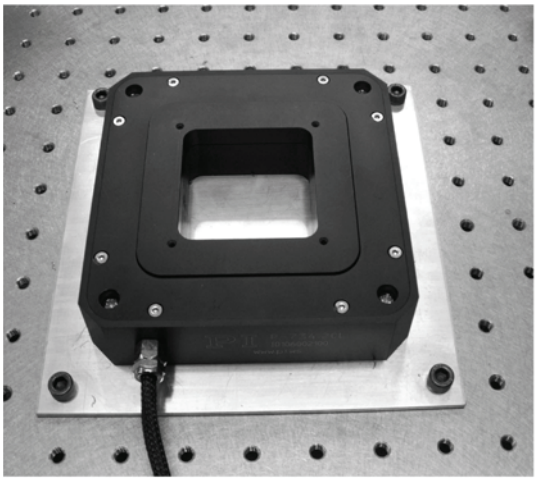

Fig. 1. The commercially available P-734 X-Y nanopositioning platform from Physik Instrumente bolted to a pneumatic isolation table.

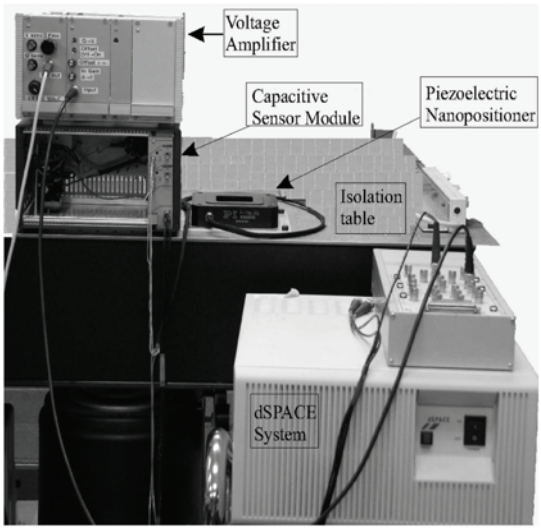

Fig. 2. A snapshot of the experimental setup used in this work

2. EXPERIMENTAL STEUP

The P-734 nanopositioning platform, used in this work, is a two-axis piezoelectric stack-actuated platform based on a parallel-kinematic design. A close-up of this platform bolted to an isolation table is shown in Figure 1. This design provides mounting independent orthogonality and reduced cross-coupling between the two axes. Friction and stiction are eliminated by using a flexure guidance system. To increase the range of motion whilst maintaining the sub-nanometer accuracy of the platform, it is equipped with a built-in integrated lever motion amplifier. Each axis of the nanopositioning platform is fitted with a two-plate capacitive sensor that provides a direct position measurement. The piezoelectric stack actuators take voltage input in the range of 0 V - 100 V for each axis. The resultant motion produced by the platform is within 0 μm - 100 μm. This motion is detected by the two-plate capacitive sensors and fed to an electronic sensor output module. The output of this module is within 0 V - 6.7 V.

A dSPACE-1005 rapid prototyping system equipped with 16-bit ADC (DS2001) and DAC (DS2102) cards is used to implement the proposed strategy. The sampling frequency of this system is 40 kHz. The voltage amplifier is calibrated to have a gain of 21.

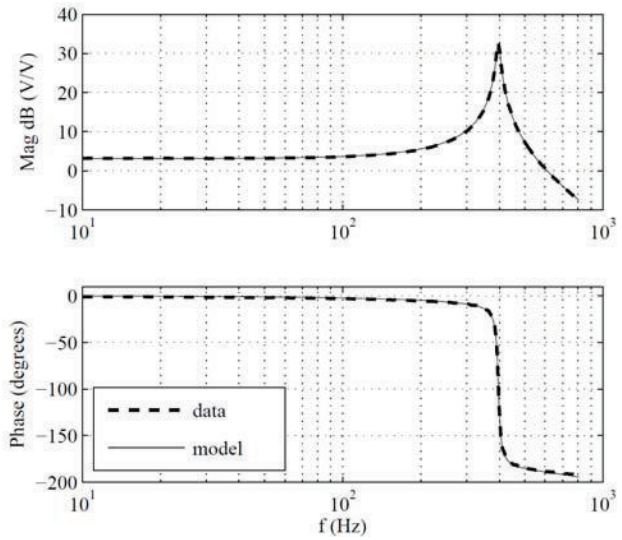

Fig. 3. Open-loop frequency response $G(j\omega)$ measured from the applied voltage to capacitive sensor output y. The frequency response of an identified model is also shown.

To measure the frequency response of one axis of the nanopositioning platform, a band-limited random noise input was generated by an HP signal analyzer, of amplitude 100 *mVpk* within the frequency range of 10 Hz - 810 Hz. This signal was fed to the voltage amplifier as input and the amplifier output was used to excite the piezoelectric stack. This input corresponds to a displacement within 0 - 2 μm, or 2% of the total range of the platform. The piezoelectric stack actuator was biased at +40 V, to avoid accidental depolarization due to application of negative voltages. The identification started 10 Hz onwards as no relevant dynamics exist in the low frequency regions (0 Hz - 10 Hz). The piezoelectric stack on the other axis is shorted out to eliminate its effect on the measurements. The input is a voltage signal applied to the piezoelectric stack (u in V), and the output is the displacement (d in μm) obtained by scaling the measured capacitive sensor voltages by the proportional scaling factor (0.067 V/μm). A picture of the complete setup is given in Figure 2. A subspace-based modeling technique, [33], is used to obtain accurate models of the open- and closed-loop system. A second-order model obtained using this method accurately captures the system dynamics in the bandwidth of interest. This procured model is used throughout this work for control design and analysis purposes.

The open-loop transfer function is plotted in Figure 3. Also plotted is an identified model procured using the frequency domain subspace technique[1]. The plant model is

$$G = \frac{0.0362s^2 - 443s + 8.83' 10^6}{s^2 + 82.4s + 6.21' 10^6} . \quad (1)$$

3. CONTROL DESIGN

The foremost control objective in nanopositioning is to minimize tracking error. As the system is non-linear, this requires integral action in the control loop. For high-speed operation the closed-loop system must be inverted either offline or with a feedforward controller. Although this is straightforward to accomplish, the resulting performance is highly sensitive to small changes in resonance frequencies. In this work, a damping controller is utilized to attenuate the systems first resonance mode. This provides improved disturbance rejection, increased gain margin and significantly reduces the performance sensitivity to changes in resonance frequency.

[1] A Matlab implementation of this algorithm is freely available by contacting the second author.

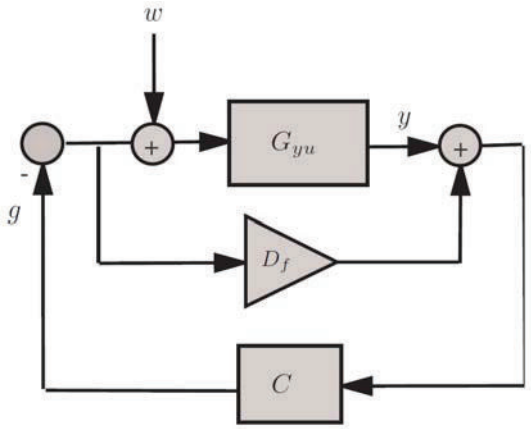

Fig. 4. Integral resonant control scheme [21]

3.1 Damping Controller

As discussed in the introduction, IRC was introduced as a means for augmenting the structural damping of resonant systems with collocated sensors and actuators. A diagram of an IRC loop is shown in Figure 4. It comprises the collocated system G_{yu}, an artificial feedthrough D_f and a controller C. The disturbance w is a force disturbance, which for the system under consideration, is equivalent to input disturbance. The first step in IRC design is to select the feedthrough term D_f. The combination of G_{yu} and D_f can then be considered a new system $G_{yu} + D_f$. By choosing D_f sufficiently large and negative, the system $G_{yu} + D_f$ contains a pair of zeros below the frequency of the first resonant mode [21]. The frequency responses of the open-loop system G and modified transfer function $G_{yu} + D_f$ are plotted in Figure 5. A key observation is that the phase of $G_{yu} + D_f$ lies between 0 and -180 degrees. Thus, a negative integral controller

$$C = \frac{-k}{s}, \quad (2)$$

adds a constant phase lead of 90 degrees to the loop gain. The phase response of the resulting loop-gain now lies between +90 and -90 degrees. That is, regardless of controller gain, the closed-loop system has a phase margin of 90 degrees. The controller gain k can easily be selected to maximize damping using the root-locus technique [21].

3.2. Tracking Controller

After implementing an IRC controller, shown in Figure 4, a secondary integral control loop cannot be directly closed around the output of G_{yu}. The feedthrough term D_f and the location of the summing junction prevent the possibility for integral action. To incorporate an additional control loop, the feedback diagram must be rearranged so that an additional input does not appear as a disturbance. This can be achieved by finding an equivalent regulator that provides the same loop gain but with an input suitable for tracking control. In Figure 4, the control input g is related to the measured output y by

$$g = C(y + gD_f), \quad (3)$$

thus, the equivalent regulator C2 is

$$C_2 = \frac{C}{1 + CD_f}. \quad (4)$$

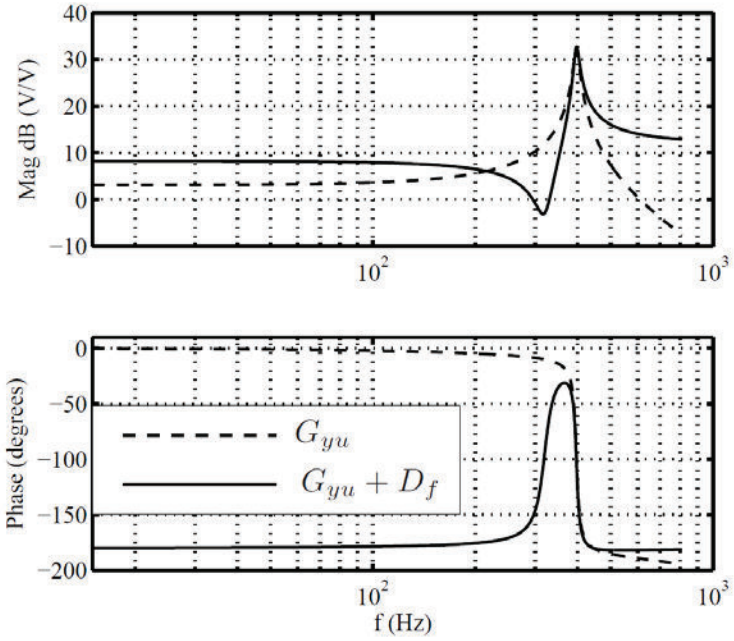

Fig. 5. Frequency response of G_{yu} and $G_{yu} + D_f$, where $D_f = -4$.

When $C = \frac{-k}{s}$, the equivalent regulator is

$$C_2 = \frac{-k}{s - kD_f}. \quad (5)$$

A diagram of the equivalent regulator loop formed by C_2 and G is shown in Figure 4. This loop is easily enclosed in a secondary outer loop to achieve integral tracking. A control diagram of this configuration is shown in Figure 7. Due to the inverting behavior of the IRC loop, the tracking controller C_3 is a negative integral controller

$$C_3 = \frac{-k_i}{s}. \quad (6)$$

The transfer function of the closed-loop system is $\frac{y}{r} = \frac{-C_3G_3}{1 + C_3G_3}$, (7)

where G_3 is the complimentary sensitivity of the IRC control loop,

$$G_3 = \frac{C_2G_{yu}}{1 + C_2G_{yu}}. \quad (8)$$

In addition to the closed-loop response, the transfer function from disturbance to the regulated variable y is also of importance. This can be found as

$$\frac{y}{w} = \frac{G_{yu}}{1 + C_2G_{yu}(1 + C_3)}. \quad (9)$$

That is, the disturbance input is regulated by the equivalent controller $C_2(1 + C_3)$. In the following section, results from implementing the proposed control scheme on the P-734 nanopositioner will be presented.

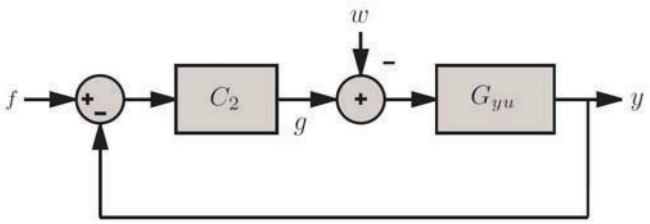

Fig. 6. The integral resonant controller of Figure 4 rearranged in regulator form

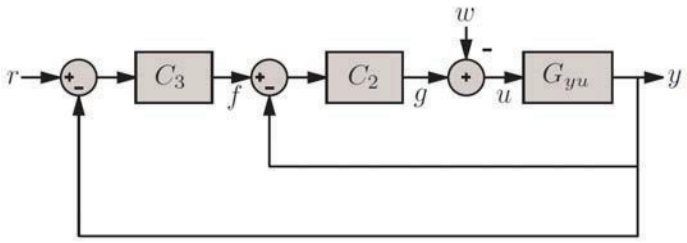

Fig. 7. Tracking control system with the damping controller $C_2(s)$ and tracking controller $C_3(s)$

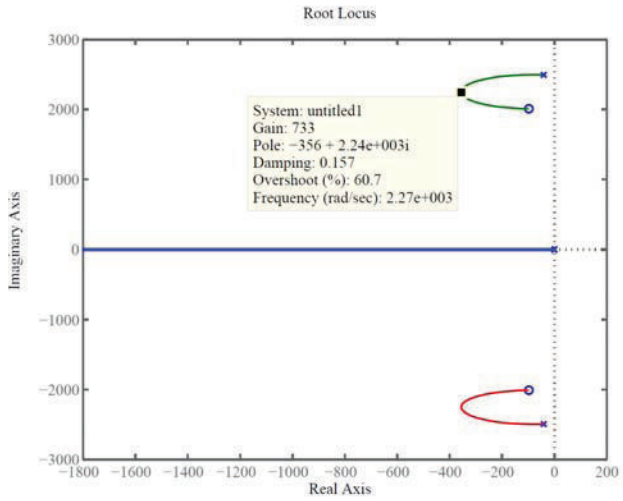

Fig. 8. Root-locus plot showing the necessary gain, resulting damping and the trajectory of the resonant pole with respect to system gain.

4. RESULTS

A brief description of the implemented controllers and the corresponding gains is given. The measured open and closed loop frequency responses for G_{yr} and G_{yw} were recorded using an HP signal analyzer. The control strategy was implemented using a dSPACE-1005 rapid prototyping system equipped with 16-bit ADC (DS2001) and DAC(DS2102) cards with a sampling frequency of 40 kHz.

4.1. Damping Controller Design

Based on the plant model G_{yu} (1), a feedthrough term of $D_f = -4$ is sufficient to produce a pair of low-frequency zeros in $G_{yu} + D_f$. By applying the root-locus technique to the loop-gain $\frac{-1}{s}(G_{yu} + D_f)$, a gain of $k = 733$ results in maximum damping performance, see Figure 8.

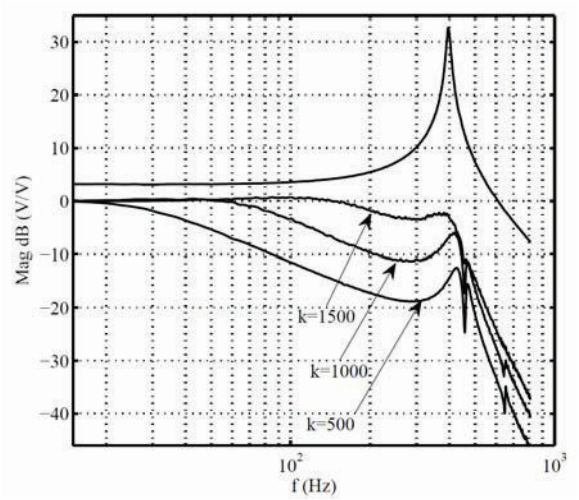

Fig. 9. The closed-loop frequency response measured from the reference input r to the displacement y measured as an equivalent voltage by the capacitive sensor.

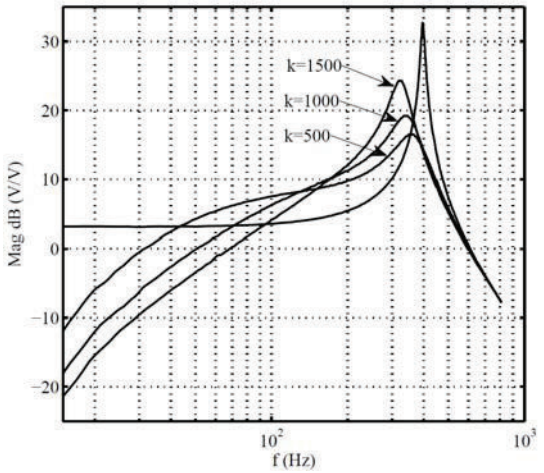

Fig. 10. The closed-loop disturbance rejection measured from *w* to the displacement *y* measured as an equivalent voltage by the capacitive sensor.

The corresponding regulator C_2 is

$$C_2 = \frac{-733}{s + 2329}. \quad (10)$$

4.2. Tracking Controller Design

Three different integral tracking controllers were implemented. The controller gain and corresponding stability margins are tabulated below.

k_i	Gain margin	Phase margin
500	12 dB	80°
1000	5.5 dB	69°
1500	2.0 dB	57°

4.3. Experimental Response

The closed loop frequency responses from the reference input *r* to the displacement *y* is plotted for each controller gain in Figure 9. A well regulated bandwidth proportionate to the controller gain is

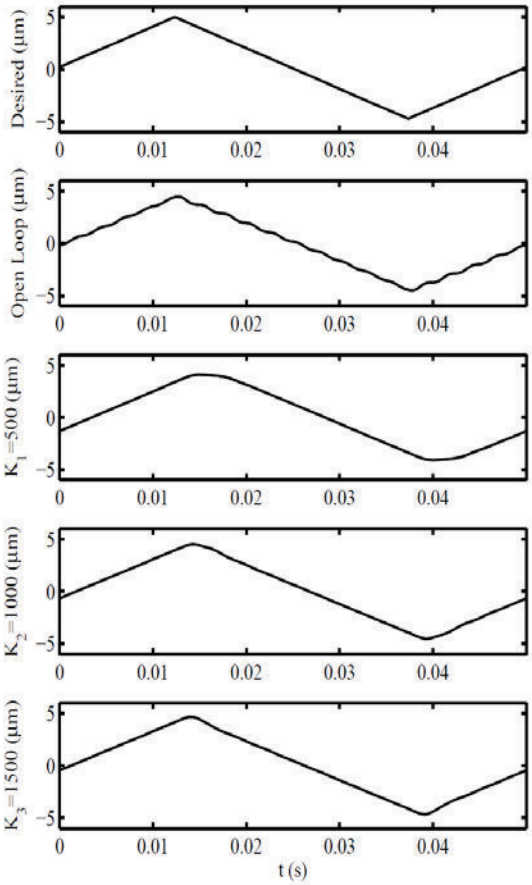

Fig. 11. The open- and closed-loop response to a 20 Hz 10 μm triangle wave. The desired output and open-loop response are plotted first, followed by the closed-loop responses for increasing values of k_i.

observed. The response to disturbance is also plotted in Figure 10. At low frequencies, there is a substantial improvement in the disturbance rejection profile exhibited by the closed-loop system. At high tracking controller gains, the disturbance rejection provided by the damping controller is reduced by the tracking controller. Depending on the application specific performance criteria, an adequate gain can be chosen to give the desired tracking bandwidth and disturbance rejection.

The time domain tracking performance was evaluated by applying a voltage that will produce a 20 Hz 10 μm triangular platform displacement. The capacitive sensor output is recorded and the corresponding displacement for each controller gain is plotted in Figure 11. In open-loop, it is clearly seen that the high-frequency harmonic components of the triangle wave excite the platform resonance and thus introduce substantial errors in the output trace. As seen from the closed- loop traces, the damping imparted by the IRC scheme is substantial and the errors due to high frequency harmonics are suppressed. Increasing the gain of the tracking controller increases the bandwidth, visible from the accuracy (sharpness) with which the extremities of the triangle wave are traced.

5. CONCLUSIONS

The controller performs well, is only second order and has excellent stability margins. It can be implemented with a simple analog circuit, one first-order low-pass filter and one integrator. Due to the damping imparted to the system in closed loop, the system is less sensitive to resonance frequency changes. This favorable condition can be further exploited to remove tracking lag by using feedforward inversion based techniques. Due to the simplicity and stability of the proposed

control algorithm and resulting improvement in tracking performance, this can be easily incorporated in control modules of most popular nanopositioning systems.

REFERENCES

1 Bhushan, *Handbook of Micro/Nanotribology*, 2nd ed. Boca Raton, USA: CRC, 1999.
2 G. Binnig and H. Rohrer, "The scanning tunneling microscope," *Scientific American*, vol. 253, pp. 50–56, 1986.
3 M.Scott, "MEMS and MOEMS for national security applications Reliability, testing and characterization of MEMS/MOEMS II," ser. 4980, SPIE, Bellingham, 2003.
4 G. Requicha, S. Meltzer, F. P. T. Arce, J. H. Makaliwe, H. Sikn, S. Hsieh, D. Lewis, B. E. Koel, and M. E. Thompson, "Manipulation of nanoscale components with the afm: Principles and applications," *Proceedings of the 1st IEEE Conference on Nanotechnology, Maui, Hawaii USA, October*, pp. 81 – 86, 2001.
5 T. Ando, N. Kodera, D. Maruyama, E. Takai, K. Saito, and A. Toda, "A high-speed atomic force microscope for studying biological Macromolecules in action," *Japanese Journal of Applied Physics*, vol. 41, no. 7B, pp. 4851–4856, 2002.
6 S. Devasia, E. Eleftheriou, and R. Moheimani, "A survey of control issues in nanopositioning," *IEEE Trans. on Control Systems Technology: Special Issue on Dynamics and Control of Micro- and Nanoscale Systems.*, vol. 15, no. 5, pp. 802 – 823, September 2007.
7 Fujimasa, *Micromachines: A New Era in Mechanical Engineering*. Oxford, UK.: Oxford University Press, 1996.
8 "PI-734 datasheet," *Physik Instrumente Catalogue*, 2007.
9 *Nano-PDQ series, Mad City Labs Inc.*, 2007.
10 S. S. Aphale, B. Bhikkaji, and S. O. R. Moheimani, "Minimizing scanning errors in piezoelectric stack-actuated nanopositioning platforms," *IEEE Trans. on Nanotechnology*, vol. 7, no. 9, pp. 79 – 90, 2008.
11 J. Fleming and S. O. R. Moheimani, "Adaptive piezoelectric shunt damping," *IOP Smart Materials and Structures*, vol. 12, pp. 18 – 28, February 2003.
12 D. Niederberger, A. J. Fleming, S. O. R. Moheimani, and M. Morari, "Adaptive multimode resonant piezoelectric shunt damping," *Smart Materials and Structures*, vol. 18, no. 2, pp. 291–315, October 2004.
13 Kang and J. K. Mills, "Vibration control of a planar parallel manipulator using piezoelectric actuators," *J. Intell. Robotics Syst.*, vol. 42, no. 1, pp. 51–70, 2005.
14 G. Schitter, P. Menold, H. Knapp, F. Allgower, and A. Stemmer, "High performance feedback for fast scanning atomic force microscopes,," *Rev. Sci. Instrum.*, vol. 72, no. 8, pp. 3320 – 3327, 2001.
15 N. Kodera, H. Yamashita, and T. Ando, "Active damping of the scanner for high-speed atomic force microscopy," *Rev. Sci. Instrum.*, vol. 76, no. 5, pp. 1 – 5, 2005.
16 H. R. Pota, S. O. R. Moheimani, and M. Smith, "Resonant controllers for smart structures," *Smart Materials and Structures*, vol. 11, no. 1, pp. 1 – 8, 2002.
17 J. L. Fanson and T. K. Caughey, "Positive position feedback control for large space structures," *AIAA Journal*, vol. 28, no. 4, pp. 717 – 724, 1990.
18 G. C. Goodwin, S.F. Graebe and M. E. Salgado, *Control System Design*. Prentice Hall International, Inc, 2001.
19 S. O. R. Moheimani, B. J. G. Vautier, and B. Bhikkaji, "Experimental implementation of extended multivariable PPF control on an active structure," *IEEE Trans. Contr. Syst. Tech.*, vol. 14, no. 3, pp. 443–455, May 2006.
20 Bhikkaji, M. Ratnam, A. J. Fleming, and S. O. R. Moheimani, "High-performance control of piezoelectric tube scanners." *IEEE Trans. Control Systems Technology*, vol. 5, no. 5, pp. 853 – 866, September 2007.

21 S. S. Aphale, A. J. Fleming, and S. O. R. Moheimani, “Integral resonant control of collocated smart structures,” *Smart Materials and Structures*, vol. 16, pp. 439 – 446, 2007.
22 M. Tomizuka, “On the design of digital tracking controllers,” *ASME Journal of Dynamic Systems, Measurement and Control*, pp. 412 – 418, November 50th Anniversary Issue.
23 Tsao, “Optimal feedforward digital tracking controller design,” *ASME Journal of Dynamic Systems, Measurement and Control*, vol. 116, no. 4, pp. 583 – 592, December 1994.
24 Q. Zhou and S. Devasia, “Preview-based optimal inversion for output tracking: Application to scanning tunneling microscopy,” *IEEE Trans. on Control System Technology*, vol. 12, no. 3, pp. 375 – 386, May 2004.
25 Croft, S. Stilson, and S. Devasia, “Optimal tracking of piezo-based nanopositioners,” *Nanotechnology*, vol. 10, no. 2, pp. 201 – 208, June 1999.
26 Croft, G. Shedd, and S. Devasia, “Creep, hysteresis, and vibration compensation for. piezoactuators: Atomic force microscopy application,” *Journal of Dynamic Systems, Measurement, and Control*, vol. 123, no. 1, pp. 35–43, March 2001.
27 Y. Zhao and S. Jayasuriya, “Feedforward controllers and tracking accuracy in the presence of plant uncertainties,” *Trans. of ASME, Journal of Dynamic Systems, Measurement and Control*, vol. 117, pp. 490 – 495, December 1995.
28 S. Salapaka, A. Sebastin, J. P. Cleveland, and M. V. Salapaka, “High bandwidth nano-positioner: A robust control approach,” *Review of Scientific Instruments*, vol. 73, no. 9, p. 3232 3241, 2002.
29 M. Sitti and H. Hashimoto, “Teleoperated tough feedback from the surfaces at the nanoscale: Modeling and experiments,” *IEEE/ASME Trans. on Mechatronics*, vol. 8, pp. 287 – 298, February 2003.
30 Sebastian and S. M. Salapaka, “Design methodologies for robust nano-positioning,” *IEEE Trans. Contr. Syst. Tech.*, vol. 13, no. 6, pp. 868 – 876, November 2005.
31 S. O. R. Moheimani, S. Devasia, and E. Eleftheriou, “Guest editorial introduction to the special issue on dynamics and control of micro and nanoscale systems,” *IEEE Trans. on Control Systems Technology*, vol. 15, no. 5, pp. 799 – 801, 2007.
32 S. S. Aphale, S. Devasia, and S. O. R. Moheimani, “High-bandwidth control of a piezoelectric nanopositioning stage in the presence of plant uncertainties,” *Nanotechnology*, vol. 19, p. 125503 (9pp), 2008.
33 T. McKelvey, H. Akcay, and L. Ljung, “Subspace based multivariable system identification from frequency response data,” *IEEE Trans. On Automatic Control*, vol. 41, no. 7, pp. 960–978, July 1996.